A Dual-Point Technique for the Entire I_D–V_G Characterization Into Subthreshold Region Under Random Telegraph Noise Condition

Xuepeng Zhan, Chengda Shen, Zhigang Ji, *Member, IEEE*, Jiezhi Chen, *Senior Member, IEEE,* Hui Fang, Fangbin Guo, and Jianfu Zhang

Abstract—**A simple dual-point technique to measure the entire transfer characteristics (I_D–V_G) down to sub-threshold region in the nano-scaled MOSFET under random telegraph noise (RTN) condition with either capturing or emitting one elementary charge by a trap in the gate dielectric is proposed. Its compatibility with the commercial semiconductor analyzer makes it a readily-usable tool for future RTN study. In this letter, we use this technique to explore the V_G dependence of RTN induced by a single trapped carrier in both n- and p-FETs.**

Index Terms—**Random telegraph noise(RTN), reliability, bias temperature instability, time-dependent variability.**

I. INTRODUCTION

RANDOM Telegraph Noise (RTN) has become one standard test for future ultra-scaled transistors [1]–[3]. However, the standard RTN procedure [4] only captures the current under constant gate voltage, V_{G_RTN}, which contains limited information. Understanding the entire I_D–V_G curve and its shift induced by the Random Telegraph Noise (RTN) can provide valuable information in understanding its underlying physical mechanism [5]–[7] and also in the circuit simulation for the time-dependent variability prediction [8], [9]. Usually such measurement is carried out by repeating the standard RTN test procedure under different V_G levels [10], [11]. However, most RTNs are only clear

in narrow voltage range [12], such method cannot probe a broad range of I_D–V_G. Recently, Franco *et al.* [13] tackled this problem by sweeping the entire I_D–V_G immediately after the RTN test. However, such method requires the rigorous selection of devices that contain only one individual defect with very slow characteristic time and with giant magnitude. This makes the method inapplicable to most of the samples. The recent Trigger-When-Charged method [14] exploited the oscilloscope-based fast-measurement system in which the edge of RTN is used to trigger the entire I_D–V_G measurement. But the method requires the dedicated configuration to reduce the background noise. Moreover, the use of the oscilloscope limits the measurement accuracy. Existing RTN models calculate the V_G dependence of the RTN magnitude theoretically with assumptions, which introduce the inaccuracy for the prediction of RTN-induced noise and their impact in circuits [15]. Therefore, a generic but straightforward characterization technique is urgently required. *In this letter, for the first time, we propose a Dual-Point method to fill this gap*. The method captures the entire I_D–V_G down to subthreshold region under RTN condition with any individual trap of characteristic time longer than $1\mu s$. This method can be directly deployed in the commercial semiconductor analyzer, making it possible to be used as the standard RTN measurement.

II. DUAL-POINT CHARACTERIZATION TECHNIQUE

The gate stack of the MOSFETs uses SiO_2 for interlayer, HfO_2 for HK layer, and TiN for work function metal. The equivalent oxide thickness is 1.65 nm. Unless specified, the devices under test have a channel length/width of 70 nm/90 nm and are all tested under room temperature with drain voltage of 100mV [16]. Keithley 4200 is used for the measurement with the same connection as the standard fast I_D–V_G configuration: two pulse units are connected with the Gate and Drain while the source and the substrate are grounded. nFETs are used for the demonstration of the technique and both n- and p- FETs are used for the exploration of RTN magnitude.

Capturing the entire I_D–V_G during RTN requires fast speed that can freeze the trap either in its charged or empty state during the measurement. Due to the low bandwidth in the commercial equipment, the speed for I_D–V_G measurement at the pulse edge is usually longer than $20\mu s$ [16]. Moreover, only linear region can be captured due to the poor accuracy. Single-point measurement [17] is an alternative to shorten the measurement time to $\sim 1\mu s$ while maintaining reasonable
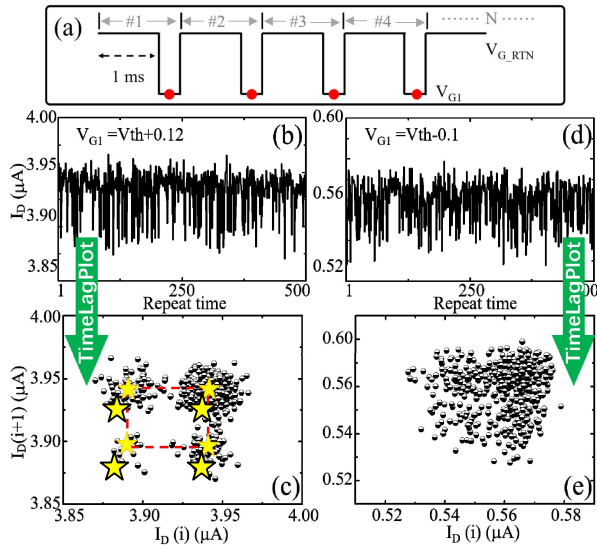
Fig. 1. **(a)** Gate voltage waveform for measuring RTN-induced current variation at V_{G1}, that is different from the voltage used for RTN test under V_{G_RTN}. Currents are measured at **(b)** V_{G1} =0.76V ($> V_{th}$) and **(d)** V_{G1} =0.54V ($< V_{th}$) after the RTN test under V_{G_RTN} =0.65V. The corresponding time-lag plot are shown in **(c)** and **(e)** respectively. The measurement time, t_m, of 10 μs is used.

Fig. 2. **(a)** The waveform for the proposed Dual-Point technique. I_D are measured at V_{GL} and V_{GH}. Two typical RTN results under V_{G_RTN} = 0.8V are shown in **(b)** and **(c)** where the current ends with low or high levels randomly. **(d)**The relationship between I_D at V_{GL} =0.52V and V_{GH} = 1.10V after RTN test under V_{G_RTN} = 0.8V. Wherein, one point corresponds to one Dual-Point measurement. In total, 500 measurements are repeated. t_m, of 500ns is used.

accuracy, as shown in **Fig. 1a**. **Fig. 1b** shows one typical result measured in linear region ($V_{G1} > V_{th}$). The RTN-induced current variation, ΔI_D, can be clearly observed with time-lag plot [18]. However, when lowering V_{G1} into subthreshold ($V_{G1} < V_{th}$), ΔI_D becomes too small to be differentiated, as shown in **Fig. 1d&e**.

We propose a Dual-Point method to tackle this problem. The new method guarantees the fast measurement speed while achieving high accuracy, which allows the I_D–V_G measurement into subthreshold region under RTN condition.

Fig.2a shows the waveform of V_G for the proposed method: After performing the standard RTN test under V_{G_RTN} for a very short time (1ms in this work), V_G is altered to V_{GL} and then V_{GH} sequentially, in which the drain currents will be measured at each level. At the end of the RTN test, due to its stochastic nature, the single trap will either capture (**Fig.2b**) or emit (**Fig.2c**) one charge carrier and accommodate itself into the charged or empty state. When the follow-on dual-point measurements are fast enough, the charging state of the individual trap will not change: The currents at V_{GL} and V_{GH} with the trap in its charged state will always be smaller than the corresponding currents measured with the trap in its empty state. **Fig. 2d** shows one typical result by repeating for multiple times. The currents under V_{GL} is plotted against the values under V_{GH}. Two clear clusters can be observed suggesting the two states of the trap. In practice, it is possible that the charging state of the trap can change during the measurement. If this happens, the point will lie out of those two clusters. This is rare as confirmed in **Fig.2d**. The centroid of each cluster represents the currents under V_{GL} or V_{GH} with the trap in both charged and empty state. We used the iterative k-means clustering algorithm [19] to automate the centroid identification, that also helps minimize the impact of outliners for better accuracy. To capture the entire I_D–V_G, we repeated the test procedure by fixing V_{GH} at operating condition and sweeping V_{GL} from subthreshold region to the linear region.
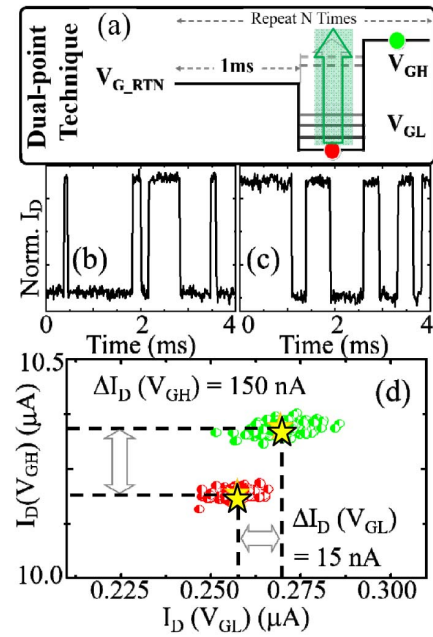
What is worth noting is that since this method freezes the trapping state during the measurement, it is limited to the RTN magnitude extraction. No timing characteristic of the trap (such as capture and emission time) can be extracted.

What is worth noticing is that ΔI_D of $\sim$15nA at V_{GL} has been clearly separated. Such success is because the proposed method measures currents at both V_{GL} and V_{GH}, and plotted them against each other. Towards the vertical and horizontal directions, ΔI_D represents the current variation in V_{GH} and V_{GL} respectively, $\Delta I_D(V_{GH})$ and $\Delta I_D(V_{GL})$. Recent results [20] confirm that ΔI_D in linear region is much larger than in subthreshold region. Therefore, the large gap in vertical direction created by $\Delta I_D(V_{GH})$ makes the two clusters distinguishable even there is tiny gap in the horizontal direction.

The measurement time for each point, t_m, is further explored. Shorter t_m increases the chance to freeze the trap during measurement. Moreover, it also reduce the possibility in charging up extra traps at higher voltage level. For simplicity but without loss of generality, we use the current measured at V_{GL} for the discussion. **Fig.3a&b** show the average value (μ_I_D) and the variation (σ_I_D). μ_I_D determines the accuracy of the method. As shown in **Fig.3a**, μ_I_D at the charged and empty state keep constant until t_m reduces to 500ns. When t_m further decreases, μ_I_D starts to rise. This is because t_m is shorter than the settle time that V_G is not yet lowered down to V_{GL}. Such speed ensures the method can be applied on RTN traps with the characteristic time larger than $\sim$1μs. The corresponding σ_I_D are shown in **Fig.3b**, which increases monotonically with shorter t_m. However, σ_I_D will not limit the measurement resolution of the proposed method. With the speed of 500ns, σ_I_D is $\sim$25nA. This guarantees the separation with ΔI_D over $\sim$50nA, that can be met by most
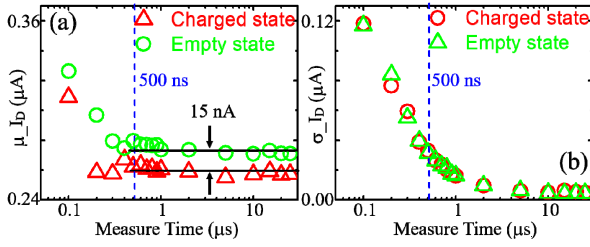
Fig. 3. The impact of the measurement time, t_m, on **(a)** the average value and **(b)** the standard deviation of I_D.
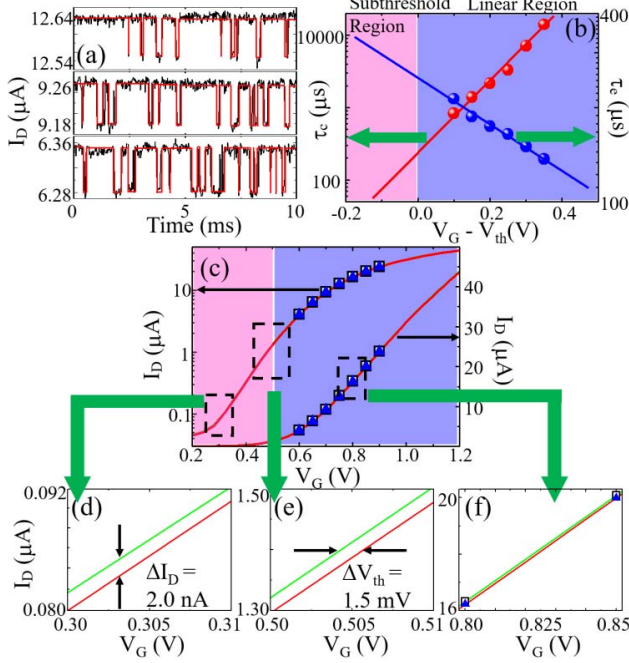

Fig. 4. **(a)** RTN measurement under constant voltage from 0.75V to 0.65V downwards with a step of 0.05V. Both the magnitude and the capture/emission time are extracted with HMM fitting (red line). **(b)** V_G dependence for the capture/emission time and their extrapolation into subthreshold region. **(c)** The two entire I_D-V_G curves captured under the RTN condition are plotted in both linear and log scale. The current extracted from the standard RTN method is also plotted as points for comparison with the enlargement in **(f)**. The region in the subthreshold and linear domain are enlarged in **(d)** and **(e)**. The RTN-induced threshold voltage shift of ~ 1.5 mV and ΔI_D of 2nA can be clearly separated.

samples under V_{GH} in linear region. The two clusters therefore can be separated vertically even they have small difference horizontally under V_{GL}, as confirmed in **Fig.3a** that 15nA ($< \sigma\_I_D$) can be clearly separated.

Finally, **Fig.4a**–f shows one example for the RTN magnitude extraction with the proposed method. Standard RTN method can only characterize a limited range of V_G, as shown in **Fig.4a**. V_G dependence of the corresponding capture/emission time in **Fig.4b** suggests that this trap is fast: At subthreshold and linear region, the electron detrapping and trapping can occur with less than 200μs respectively. **Fig.4c** shows the extracted I_D–V_G curves using our proposed method: the two curves correspond to this single trap in the empty and charged state respectively. It is clear that both curves can be measured down to subthreshold region. As enlarged in **Fig.4d**&e, the ΔV_{th} of 1.5mV and ΔI_D of 2nA can be clearly identified with the proposed method. What is also worth noting is that within the measurement window of the standard RTN method, the two methods agree very well with each other, as enlarged
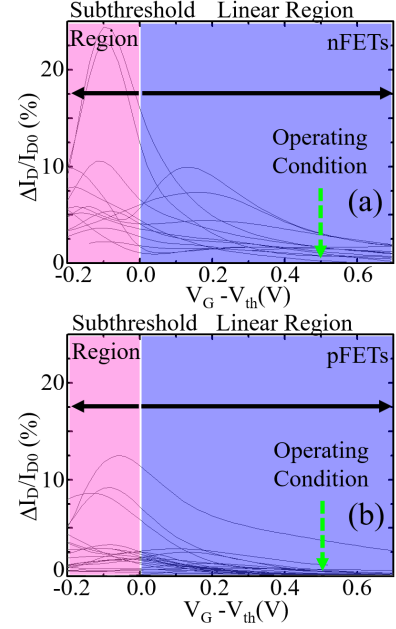

Fig. 5. Vg dependence of $\Delta I_D/I_{D0}$ induced by individual traps under RTN condition on **(a)** nFETs and **(b)** pFETs. t_m of 500ns is used.

in **Fig.4f**. However, the new method has much wider window from subthreshold to operating condition.

III. APPLICATIONS TO RTN STUDY IN NANO-SCALED DEVICE

In this section, we applied the Dual-Point method to explore the V_G dependence of the RTN magnitude. By convention**[9]**, the RTN magnitude is defined as $\Delta I_D/I_{D0}$ under constant V_G, where I_{D0} is the drain current with the single trap at its empty state. $\Delta I_D/I_{D0}$ against V_G from multiple nano-scaled p- and n- FETs are shown in **Fig.5a&b** respectively. Overall, nFET exhibits the larger $\Delta I_D/I_{D0}$ variations compared with pFETs, which agrees with some recent reports **[21], [22]**. It is not clear yet whether this is a general phenomenon and future investigations are needed. Our result also shows that $\Delta I_D/I_{D0}$ are larger around threshold region and reduce towards the operating region. This agrees well with the 3D atomic simulation results by assuming different distances between individual traps in the dielectric and the percolation path in the channel induced by the non-uniform doping **[23]**. Since the standard RTN test measures $\Delta I_D/I_{D0}$ close to threshold region, this result suggests that the time-dependent variation could be overestimated **[24]**. Therefore, the measurement of the entire I_D–V_G under the RTN condition is essential.

IV. CONCLUSION

We developed a simple Dual-Point technique that can be directly deployed in the commercial semiconductor analyzer. The accuracy and precision of the method is discussed in details. The proposed technique can be used to capture the wide range of I_D–V_G from the subthreshold region up to device operating condition. With its fast measurement speed of 500ns, the technique can be applied on most of the devices that contains single traps in the dielectric. Finally, we applied this method to evaluate the V_G dependence of the impact of a single trapped carrier in both n- and p- FETs.

REFERENCES

[1] S. Dongaonkar, M. D. Giles, A. Kornfeld, B. Grossnickle, and J. Yoon, "Random telegraph noise (RTN) in 14 nm logic technology: High volume data extraction and analysis," in *Proc. IEEE Symp. VLSI Technol.*, Jun. 2016, pp. 1–2. doi: 10.1109/VLSIT.2016.7573424.

[2] N. Tega, H. Miki, Z. Ren, C. P. D'Emic, Y. Zhu, D. J. Frank, M. A. Guillorn, D.-G. Park, W. Haensch, and K. Torii, "Impact of HK/MG stacks and future device scaling on RTN," in *Proc. Int. Rel. Phys. Symp. (IRPS)*, Apr. 2011, pp. 6A.5.1–6A.5.6. doi: 10.1109/IRPS.2011.5784546.

[3] L. Pirro, O. Zimmerhackl, A. Zaka, L. Miiller-Meskamp, R. Nelluri, T. Hermann, I. Cortes-Mayol, A. Huschka, M. Otto, E. Nowak, A. Mittal, and J. Hoentschel, "RTN and LFN noise performance in advanced FDSOI technology," in *Proc. 48th Eur. Solid-State Device Res. Conf. (ESSDERC)*, Sep. 2018, pp. 254–257. doi: 10.1109/ESSDERC.2018.8486917.

[4] M. J. Uren, D. J. Day, and M. J. Kirton, "1/f and random telegraph noise in silicon metal-oxide-semiconductor field-effect transistors," *Appl. Phys. Lett.*, vol. 47, no. 11, pp. 1195–1197, Sep. 1985. doi: 10.1063/1.96325.

[5] K. P. Cheung and J. P. Campbell, "On the magnitude of random telegraph noise in ultra-scaled MOSFETs," in *Proc. IEEE Int. Conf. IC Design Technol. (ICICDT)*, May 2011, pp. 1–4. doi: 10.1109/ICICDT.2011.5783191.

[6] C. Chen, Q. Huang, J. Zhu, Y. Zhao, L. Guo, and R. Huang, "New understanding of random telegraph noise amplitude in tunnel FETs," *IEEE Trans. Electron Devices*, vol. 64, no. 8, pp. 3324–3330, Aug. 2017. doi: 10.1109/TED.2017.2712714.

[7] I. Zadorozhnyi, J. Li, S. Pub, H. Hlukhova, V. Handziuk, Y. Kutovyi, M. Petrychuk, and S. Vitusevich, "Effect of gamma irradiation on dynamics of charge exchange processes between single trap and nanowire channel," *Small*, vol. 14, no. 2, Jan. 2018, Art. no. 1702516. doi: 10.1002/smll.201702516.

[8] M. Luo, R. Wang, S. Guo, J. Wang, J. Zou, and R. Huang, "Impacts of random telegraph noise (RTN) on digital circuits," *IEEE Trans. Electron Devices*, vol. 62, no. 6, pp. 1725–1732, Jun. 2015. doi: 10.1109/TED.2014.2368191.

[9] M.-L. Fan, S.-Y. Yang, V. P.-H. Hu, Y.-N. Chen, P. Su, and C.-T. Chuang, "Single-trap-induced random telegraph noise for FinFET, Si/Ge Nanowire FET, tunnel FET, SRAM and logic circuits," *Microelectron. Rel.*, vol. 54, no. 4, pp. 698–711, Apr. 2014. doi: 10.1016/j.microrel.2013.12.026.

[10] K. K. Hung, P. K. Ko, C. Hu, and Y. C. Cheng, "Random telegraph noise of deep-submicrometer MOSFETs," *IEEE Electron Device Lett.*, vol. 11, no. 2, pp. 90–92, Feb. 1990. doi: 10.1109/55.46938.

[11] J. Brown, R. Gao, Z. Ji, J. Chen, J. Wu, J. Zhang, B. Zhou, Q. Shi, J. Crowford, and W. Zhang, "A low-power and high-speed true random number generator using generated RTN," in *Proc. IEEE Symp. VLSI Technol.*, Jun. 2018, pp. 95–96. doi: 10.1109/VLSIT.2018.8510671.

[12] C.-Y. Chen, Q. Ran, H.-J. Cho, A. Kerber, Y. Liu, M.-R. Lin, and R. W. Dutton, "Correlation of Id- and Ig-random telegraph noise to positive bias temperature instability in scaled high-k/metal gate n-type MOSFETs," in *Proc. Int. Rel. Phys. Symp.*, Apr. 2011, pp. 3A.2.1–3A.2.6. doi: 10.1109/IRPS.2011.5784475.

[13] J. Franco, B. Kaczer, M. Toledano-Luque, P. J. Roussel, J. Mitard, L.-Å. Ragnarsson, L. Witters, T. Chiarella, M. Togo, N. Horiguchi, G. Groeseneken, M. F. Bukhori, T. Grasser, and A. Asenov, "Impact of single charged gate oxide defects on the performance and scaling of nanoscaled FETs," in *Proc. IEEE Int. Rel. Phys. Symp. (IRPS)*, Apr. 2012, pp. 5A.4.1–5A.4.6. doi: 10.1109/IRPS.2012.6241841.

[14] A. Manut, R. Gao, J. F. Zhang, Z. Ji, M. Mehedi, W. D. Zhang, V. David, A. Asenov, and B. Kaczer, "Trigger-when-charged: A technique for directly measuring RTN and BTI-induced threshold voltage fluctuation under use-V$_{dd}$," *IEEE Trans. Electron Devices*, vol. 33, no. 3, pp. 1482–1488, Mar. 2019.

[15] J. S. Kolhatkar, E. Hoekstra, C. Salm, A. P. van der Wel, E. A. M. Klumperink, J. Schmitz, and H. Wallinga, "Modeling of RTS noise in MOSFETs under steady-state and large-signal excitation," in *IEDM Tech. Dig.*, Dec. 2004, pp. 759–762. doi: 10.1109/IEDM.2004.1419283.

[16] Z. Ji, D. Linten, R. Boschke, G. Hellings, S. H. Chen, A. Alian, D. Zhou, and Y. Mols, T. Ivanov, J. Franco, B. Kaczer, X. Zhang, R. Gao, J. F. Zhang, W. Zhang, N. Collaert, and G. Groeseneken, "ESD characterization of planar InGaAs devices," in *Proc. IEEE Int. Rel. Phys. Symp.*, Apr. 2015, pp. 3F.1.1–3F.1.7. doi: 10.1109/IRPS.2015.7112719.

[17] R. Wang, J. Zou, X. Xu, C. Liu, J. Liu, H. Wu, Y. Wang, and R. Huang, "New observations on the AC random telegraph noise (AC RTN) in nano-MOSFETs," in *Proc. VLSI Technol., Syst. Appl.*, Apr. 2012, pp. 1–2. doi: 10.1109/VLSI-TSA.2012.6210146.

[18] T. Nagumo, K. Takeuchi, S. Yokogawa, K. Imai, and Y. Hayashi, "New analysis methods for comprehensive understanding of random telegraph noise," *IEDM Tech. Dig.*, Dec. 2009, pp. 1–4. doi: 10.1109/IEDM.2009.5424230.

[19] G. Gan and M. K.-P. Ng, "k-means clustering with outlier removal," *Pattern Recognit. Lett.*, vol. 90, pp. 8–14, Apr. 2017. doi: 10.1016/j.patrec.2017.03.008.

[20] N. Tega, H. Miki, Z. Ren, C. P. D'Emic, Y. Zhu, D. J. Frank, M. A. Guillorn, D. -G. Park, W. Haensch, and K. Torii, "Impact of HK/MG stacks and future device scaling on RTN," in *Proc. Int. Rel. Phys. Symp. (IRPS)*, Apr. 2011, pp. 6A.5.1–6A.5.6. doi: 10.1109/IRPS.2011.5784546.

[21] A. Whitcombe, S. Taylar, M. Denham, V. Milovanović, and B. Nikolić, "On-chip I–V variability and random telegraph noise characterization in 28 nm CMOS," in *Proc. Eur. Solid-State Device Res. Conf. (ESSDERC)*, Sep. 2016, pp. 248–251. doi: 10.1109/ESSDERC.2016.7599632.

[22] S. Dongaonkar, M. D. Giles, A. Kornfeld, B. Grossnickle, and J. Yoon, "Random telegraph noise (RTN) in 14 nm logic technology: High volume data extraction and analysis," in *Proc. IEEE Symp. VLSI Technol.*, Jun. 2016, pp. 978–979. doi: 10.1109/VLSIT.2016.7573424.

[23] R. Wang, S. Guo, Z. Zhang, Q. Wang, D. Wu, J. Wang, and R. Huang, "Too Noisy at the Bottom? —Random telegraph noise (RTN) in advanced logic devices and circuits," in *IEDM Tech. Dig.*, Dec. 2018, pp. 17.2.1–17.2.4. doi: 10.1109/IEDM.2018.8614594.

[24] T. Komawaki, M. Yabuuchi, R. Kishida, J. Furuta, T. Matsumoto, and K. Kobayashi, "Circuit-level simulation methodology for random telegraph noise by using verilog-AMS," in *Proc. IEEE Int. Conf. IC Design Technol. (ICICDT)*, May 2017, pp. 1–4. doi: 10.1109/ICICDT.2017.7993526.